Using intrusive approaches as a step towards accounting for stochasticity in wind turbine design

Journal of Physics: Conference Series **2767** (2024) 082001 doi:10.1088/1742-6596/2767/8/082001

Using intrusive approaches as a step towards accounting for stochasticity in wind turbine design

E. Branlard[1], C. Frontin[2], J. Maack[2], D. Laird[2]

[1]University of Massachusetts, Amherst, MA, USA
[2]National Renewable Energy Laboratory, Golden, CO, USA

E-mail: ebranlard@umass.edu

Abstract. Current wind turbine design methods require tens of thousands of time-domain simulations and use different random seeds to account for the stochasticity of the environmental conditions. The account of stochasticity is nonintrusive because the sampling method calls a deterministic model multiple times without changing its underlying equations. In this work, we investigate and demonstrate using simple proof of concepts how intrusive approaches can be used to directly account for stochasticity in the equations representing a mechanical system. Our long term goal is to apply such methodology to the design of wind turbines without requiring an excessive number of simulations. Intrusive methods manipulate stochastic variables directly to provide the probability density functions (PDFs) of the states and outputs at any time as functions of the PDFs of the inputs. We illustrate how different methods can be used with a reduced-order model of a wind turbine with one degree of freedom and for linear and nonlinear models. We discuss how the methods can be extended and what it will take to apply them to a level of fidelity similar to current state-of-the-art wind turbine design tools.

1. Introduction

Stochasticity is an inherent part of the design of wind energy systems: 1) The environmental conditions (wind, wave, current, etc.) contain a stochastic component by their turbulent nature, referred to as "aleatoric uncertainty," and 2) the modeling of the system, or the measurement of the system inputs and parameters, introduces stochastic errors that are referred to as "epistemic uncertainty." Both sources of uncertainties affect the design approach and the actual design of the system.

Current design methods handle uncertainty by modeling the system under a large sampled set of conditions, resulting in many simulations, at a non-negligible computational cost. The official standards [1] for the design of an offshore wind turbine require approximately 10,000 simulations. The simulations only account for aleatoric uncertainty. The methods used to quantify the epistemic uncertainties often use a similar approach by relying on the simulation of a large number of cases at varying parameters (such as Monte Carlo sampling) or by applying a simplified safety factor to try to stay within the design constraints of the system.

Such sampling methods are referred to as "nonintrusive" methods because they rely on a model with deterministic equations, and the underlying equations of the model are not changed to account for stochasticity. Design and optimization under uncertainty [2, 3, 4] are difficult to achieve using nonintrusive methods because of the prohibitive computational time they require. Additionally, we judge it unsatisfactory to use "brute-force" sampling methods to tackle an

inherently stochastic problem. Intrusive methods (see e.g., [5]), on the other hand, use stochastic variables and equations instead of deterministic equations to describe the model, and therefore directly account for stochasticity.

In this work, we investigate and demonstrate how intrusive and dedicated stochastic approaches can be used in solving the equation of a We focus on the account of aleatoric uncertainty with the goals of reducing the number of simulations carried out in the preliminary design process and allowing for accurate optimization under uncertainty. More precisely, we seek to obtain probability density functions (PDFs) of structural loads from the PDFs of the environmental inputs. To limit the scope of work, we focus on a reduced-order wind turbine model with one degree of freedom. We leave to future work the task of applying the methodology to the design of wind turbines. We study the reduced-order systems using both a linear method and a nonlinear stochastic method. We then compare the results to the traditional "brute-force" approach that uses time-domain simulations with multiple random seeds. Intrusive stochastic methods come with challenges of their own—in particular, extending the approach to larger systems and including controller dynamics. We discuss these challenges before concluding the article.

2. Methods

In this section, we present three methodologies to obtain probabilistic and statistical quantities related to a given system: stochastic linear theory, stochastic differential equation (SDE), and the Fokker-Planck equation (FPE). The treatments are general and can be applied to any dynamical system, but we will apply them to a wind energy case in Section 3.

2.1. Problem definition

We consider a dynamic system governed by a state and output equation defined as:

$$\dot{\boldsymbol{x}} = \boldsymbol{f}(\boldsymbol{x}, \boldsymbol{u}) \tag{1}$$

$$\boldsymbol{y} = \boldsymbol{g}(\boldsymbol{x}, \boldsymbol{u}) \tag{2}$$

where $\boldsymbol{x}$ describes an n-dimensional state, $\boldsymbol{u}$ describes an m-dimensional input, $\boldsymbol{y}$ describes an l-dimensional output of interest, $\boldsymbol{f}$ represents the dynamics of the system, and $\boldsymbol{g}$ maps the states and inputs to the output of interest $\boldsymbol{y}$.

2.2. Stochastic linear theory

Stochastic linear theory is a convenient tool to account for stochasticity directly in a linear system. It directly builds on top of tools used in linear theory, and under the assumption of ergodicity, it reduces to the so-called "frequency domain approaches" To apply it, we consider the linearized version of Equation 1:

$$\dot{\boldsymbol{x}} = \boldsymbol{A}\boldsymbol{x} + \boldsymbol{B}\boldsymbol{u} \tag{3}$$

$$\boldsymbol{y} = \boldsymbol{C}\boldsymbol{x} + \boldsymbol{D}\boldsymbol{u} \tag{4}$$

with state-space matrices $\boldsymbol{A} \in \mathbb{R}^{n\times n}$, $\boldsymbol{B} \in \mathbb{R}^{n\times m}$, $\boldsymbol{C} \in \mathbb{R}^{l\times n}$, $\boldsymbol{D} \in \mathbb{R}^{l\times m}$. We then use linear theory tools to relate the spectra of the inputs and outputs based on the transfer functions from inputs to state and inputs to outputs, $\mathbb{G}$ and $\mathbb{H}$, respectively:

$$\frac{\mathbb{X}(s)}{\mathbb{U}(s)} = \mathbb{G}(s) = (s\boldsymbol{I} - \boldsymbol{A})^{-1}\boldsymbol{B} \tag{5}$$

$$\frac{\mathbb{Y}(s)}{\mathbb{U}(s)} = \mathbb{H}(s) = \boldsymbol{C}(s\boldsymbol{I} - \boldsymbol{A})^{-1}\boldsymbol{B} + \boldsymbol{D} \tag{6}$$

Given the transfer functions, the double-sided autospectral density of the states, $\boldsymbol{S}_{XX}$, and outputs, $\boldsymbol{S}_{YY}$, is obtained from those of the inputs $\boldsymbol{S}_{UU}$, as [6]:

$$\boldsymbol{S}_{XX}(\omega) = \mathbb{G}^*(\mathrm{i}\omega)\boldsymbol{S}_{UU}(\omega)\mathbb{G}^T(\mathrm{i}\omega) \tag{7}$$

$$\boldsymbol{S}_{YY}(\omega) = \mathbb{H}^*(\mathrm{i}\omega)\boldsymbol{S}_{UU}(\omega)\mathbb{H}^T(\mathrm{i}\omega) \tag{8}$$

From these, the standard deviation of the signals can be obtained by integration of the autospectra. For instance, for the i-th state variable:

$$\sigma^2_{X_i} = \int_{-\infty}^{\infty} S_{XX,i}(\omega)\, d\omega \tag{9}$$

Higher statistical moments cannot be obtained in this method. Nonlinear systems and outputs can only be approximated by their linearized counterparts, which may have different statistical behaviors. Further discussions and limitations of the stochastic linear theory are found in Section 4. In this work, we have implemented an open-source Python framework [7] to readily apply the stochastic linear theory to a linear system.

2.3. Stochastic differential equation (SDE)

In the general (nonlinear) case of a stochastically forced problem, we can rewrite Equation 1 in terms of the Itô-type SDE:

$$\mathrm{d}\boldsymbol{x} = \boldsymbol{f}_{\mu}(\boldsymbol{x}, \boldsymbol{u})\,\mathrm{d}t + \boldsymbol{\Sigma}(\boldsymbol{x}, \boldsymbol{u})\,\mathrm{d}\boldsymbol{W} \tag{10}$$

where $\boldsymbol{f}_{\mu}$ represents the deterministic (or "mean drift") portion of the dynamics $\boldsymbol{f}$, $\boldsymbol{\Sigma}$ represents the stochastic portion of the dynamics, and $\mathrm{d}\boldsymbol{W}$ represents the Brownian increment (i.e., a white noise increment on $\mathrm{d}t$) that governs the stochastic component of the forcing. We will illustrate how the $\boldsymbol{f}_{\mu}$ and $\boldsymbol{\Sigma}$ functions are related to the system of equations of a mechanical systems in Section 3.

Because of the Brownian forcing ($\mathrm{d}\boldsymbol{W}$), the right-hand side of Equation 10 is continuous but not differentiable. Dedicated SDE solvers are required to time-integrate this equation because higher-frequency content is continuously uncovered by decreasing time step. As part of this study, we have used the SRIW1 SDE discretization scheme implemented in the Julia language [8] to perform direct numerical integrations of Equation 10. Results from the SRIW1 approach are not presented in this article because they are another form of "brute-force" time integration, which we are attempting to avoid in this work. The SDE formulation is yet useful as it is the first step to establish the Fokker-Planck equation of a system.

2.4. Fokker-Planck equation

One advantage of the SDE formulation (Equation 10) is that the time evolution of the PDFs of the system states can be described—given distributions of the system inputs—using the Fokker-Planck equation (FPE)[9]:

$$\frac{\partial p(\boldsymbol{x}, t)}{\partial t} = -\sum_i \frac{\partial}{\partial x_i}\left[f_{\mu,i}(\boldsymbol{x}, t)\, p(\boldsymbol{x}, t)\right] + \sum_i \sum_j \frac{\partial}{\partial x_i}\frac{\partial}{\partial x_j}\left[\mathcal{D}_{ij}(\boldsymbol{x}, t)\, p(\boldsymbol{x}, t)\right] \tag{11}$$

where $p(\boldsymbol{x}, t)$ is the probability density function of the system states as a function of time, and $\boldsymbol{\mathcal{D}} \equiv \frac{1}{2}\boldsymbol{\Sigma}\boldsymbol{\Sigma}^\top$, with $\boldsymbol{\Sigma}$ introduced in Equation 10. The integration requires discretization of the solution space of the states (e.g., $\mathbb{R}^n$ for a problem with n states). In this work, we integrate the FPE analytically when possible, or using a finite element approach otherwise. After performing the time integration of the equation, the PDFs of the system states are known at every time step. For simplicity, we assume that the PDFs of the outputs can be obtained from the PDFs of the states or that the state vector is augmented to include the outputs.

Because we are primarily interested in the steady-state value of the probability density, the solution can be simplified by setting the left-hand side of Equation 11 to zero, resulting in

an elliptic problem that can be solved using typical discretization methods for steady partial differential equations.

2.5. Steady-state Fokker-Planck equation for a linear system

The case of a linear system (Equation 3) is useful for the verification of numerical tools that integrate the Itô or Fokker-Planck equation. Further, it provides a link between the linear theory and the FPE formalism.

We assume that the solution for p in Equation 11 follows a multivariate normal distribution:

$$p(\boldsymbol{x}) = \frac{1}{(2\pi)^{n/2}\sqrt{\det \boldsymbol{\mathcal{C}}}} e^{-\frac{1}{2}\boldsymbol{x}^T \boldsymbol{\mathcal{C}}^{-1} \boldsymbol{x}} \tag{12}$$

where $\boldsymbol{\mathcal{C}}$ is the covariance matrix. We insert Equation 12 into the steady-state form of Equation 11. This operation results in a constant plus a term $\boldsymbol{x}^T \left[\frac{1}{2}(\boldsymbol{A}^T \boldsymbol{\mathcal{C}}^{-1} + \boldsymbol{\mathcal{C}}^{-1}\boldsymbol{A}) + \boldsymbol{\mathcal{C}}^{-1}\boldsymbol{\mathcal{D}}\boldsymbol{\mathcal{C}}^{-1}\right] \boldsymbol{x}$. The term in bracket must be zero in order to satisfy the equation for any $\boldsymbol{x}$. Therefore, the following Lyapunov equation is obtained [10]:

$$\boldsymbol{A}\boldsymbol{\mathcal{C}} + \boldsymbol{\mathcal{C}}\boldsymbol{A}^T + 2\boldsymbol{\mathcal{D}} = 0 \tag{13}$$

The above equation can be solved to determine the covariance matrix $\boldsymbol{\mathcal{C}}$. Therefore, the steady-state PDF of the state vector and the standard deviations of the state variables are entirely determined.

3. Proof of concept and numerical application

As part of this work, we implemented numerical tools, which, based on given input spectra, can: 1) perform brute-force time integration of a nonlinear mechanical system; 2) apply stochastic linear theory to a linear system, 3) integrate the Fokker-Planck equation using an FEM solver, 4) perform brute-force SDE integration using the SRIW1 scheme. The tools are made available as part of an opensource repository [7].

In this section, we present proofs of concept of the methods presented in Section 2. by using a reduced-order, linear model of a wind turbine with one degree of freedom. We use a simple model to provide an illustrative example of the complex methods introduced in Section 2. We choose a linear model so that the FPE methods can be compared to the stochastic linear theory directly, but we note that the direct integration of the SDE and the FPE method can be applied to nonlinear systems. First, we present how the reduced-order model is obtained before presenting numerical applications.

3.1. Wind turbine reduced-order model

We use the framework presented in previous work [11, 12] to obtain reduced-order models. The approach relies on a shape function approach to model the motion of the flexible bodies (support structure and blades) and joint coordinates to link the different bodies. In this work, we focus on a model with one degree of freedom representing the generalized tower fore-aft motion, noted q. The equations of motion reduce to a linear mass-spring-damper system (see [11]):

$$m\ddot{q} + c\dot{q} + kq = F(q, \dot{q}, t) \tag{14}$$

where m, c, and k are respectively the generalized mass, damping, and stiffness associated with the elastic degree of freedom, q, and F is the generalized force (which comes from aerodynamics, hydrodynamics, and potential nonlinear structural dynamics terms).

We further assume a linear forcing for simplicity (i.e., $F(q, \dot{q}, t) = F(t)$). In this case, the analysis in Section 2.2 can be used. For the stochastic setting, we assume a model of the form:

$$F(q, \dot{q}, t) = F(t; \eta) = F_0(t) + \sigma\eta(t) \tag{15}$$

where $F_0(t)$ represents the base forcing, with an additional white noise component η scaled by σ that represents the stochastic variability of the input force. In this case, the white noise term η (and Equation 14 by extension) are shorthand for a well-posed Brownian increment (which integrates into a well-posed differential form Itô SDE).

In the following numerical experiments, we will focus on obtaining the PDFs and statistics of the system states, and we assume that the PDFs of the outputs of interest can be computed from the PDFs of the states and inputs. We discuss this assumption in Section 4. As an example, the output corresponding to the bending moment at a given height z along the tower may be approximated to be a function of the states (q) using: $\mathcal{M}(z) \approx \ddot{q}(t)\kappa(z)EI(z)$, where κ is the curvature of the tower fore-aft shape function, and EI is the bending stiffness of the tower (see [12]).

We apply our numerical framework to the IEA 15-MW reference wind turbine, leading to the following numerical values: $m = 4.375 \times 10^5$ kg, $c = 6.31 \times 10^3$ Nm/s, $k = 1.84 \times 10^6$ N/m.

3.2. Sampling method

In this section, we use a typical sampling (brute force) method to obtain time series of forces, and then we integrate Equation 14 using a deterministic ordinary differential equation solver. In Section 3.1, the input force is assumed to be a Gaussian process. Gaussian processes (also called white noise) have an infinite-band spectrum, which makes it impossible to generate a white-noise time series and use a regular time-integrator (see Equation 10). To use a regular time-integrator[1], we assume that the input process has a cutoff white noise spectrum, namely:

$$S_{UU}(\omega) = \frac{\sigma_F^2}{(2\omega_c)}\Pi_{[-\omega_c;\,\omega_c]}(\omega) \tag{16}$$

where σ_F^2 is the variance of the force and $\Pi_{[-\omega_c;\,\omega_c]}$ is the gate function equal to 1 in the interval $[-\omega_c;\,\omega_c]$ and zero elsewhere, where ω_c is the cutoff frequency. In this example, we use a cutoff frequency of $\omega_c = 2\pi$ (1 Hz), which is considered far enough from the system frequency of 0.32 Hz as to not significantly affect the results.

We generate $N = 100$ samples of 600 s time series of force inputs from the input spectrum (Equation 16). We then use these time series as input to integrate Equation 14. An example of two samples of input force and resulting states (position and velocity), is shown on the right of Figure 1. For each time series, the statistics over the 600 s simulation are obtained. We plot the individual PDFs of the different samples, p_i and the ensemble average, p_N, in the left of Figure 1. The figure also contains results from linear theory and Fokker-Planck theory, as will be presented in subsequent sections.

3.3. Linear response theory

In this section, we apply the formalism of Section 2.2. In the linear case, Equation 14 is cast into the linear state-space equation given in Equation 3 as:

$$\dot{\boldsymbol{x}} = \boldsymbol{A}\boldsymbol{x} + \boldsymbol{B}\boldsymbol{u}, \qquad \boldsymbol{A} = \begin{bmatrix} 0 & 1 \\ -k/m & -c/m \end{bmatrix}, \quad \boldsymbol{B} = \begin{bmatrix} 0 \\ 1/m \end{bmatrix} \tag{17}$$

where $\boldsymbol{u} = \{F - F_0\}$ is the linearized input vector, and $\boldsymbol{x} = \{q - q_0, \dot{q}\}^T$ is the linearized state vector, where the subscript 0 indicates values at the operating point. Taking the steady-state equilibrium as the operating point leads to $q_0 = F_0/k$, where F_0 is the mean of $\boldsymbol{f}$. The time scale for the position and velocity are expected to be $\tau_q = \frac{c}{k}$, $\tau_{\dot{q}} = \frac{c}{m}$, and a steady-state solution

[1] One can use a dedicated SDE integrator (as discussed in Section 2.3), in which case, there is no need to cutoff the white noise spectrum. Because wind turbine simulation tools use continuous time integrators, we choose to limit ourselves to such integrators to be more representative of a typical wind turbine design scenario. As a result, we need to cutoff the input spectrum.

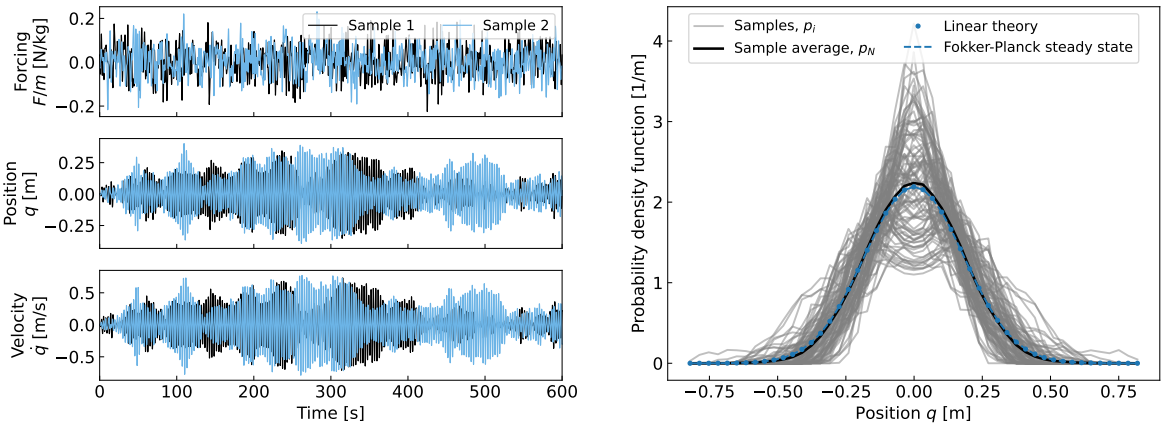

Figure 1. Left: Example of time series generated using the sampling approach. The input is the force $\boldsymbol{f}$, generated from a cutoff white-noise spectrum, and the states are the position and velocity, q and $\dot{q}$, respectively, obtained by time integration of Equation 14. Right: Probability density functions of the position as obtained using different methods: 1) sampling method, 2) linear theory, 3) steady-state Fokker-Planck method.

can be assumed if the time is sufficiently large compared to these time constants. We assume $\boldsymbol{y} = \boldsymbol{x} = \{q, \dot{q}\}^T$ for simplicity (i.e., $\boldsymbol{C} = \boldsymbol{I}$ and $\boldsymbol{D} = \boldsymbol{0}$). The transfer function is readily obtained from Equation 6, and for this simple mass-spring-damper system, a closed-form expression is obtained as [6]:

$$\frac{\mathbb{Y}(s)}{\mathbb{U}(s)} = \mathbb{H}(s) = (s\boldsymbol{I} - \boldsymbol{A})^{-1}\boldsymbol{B} = \frac{1/m}{s^2 + 2s\zeta\omega_0 + \omega_0^2}\begin{bmatrix}1\\ s\end{bmatrix} \tag{18}$$

where $\omega_0 = \sqrt{k/m}$ and $\zeta = c/\sqrt{4km}$ are the natural frequency and damping ratio, respectively. In this example, $\mathbb{H} = \{H_Q, H_{\dot{Q}}\}^T$ has dimension 2×1. The amplitudes and phases of the two components of the transfer function $\mathbb{H}(i\omega)$ are illustrated in the Bode plot provided in Figure 2. The autospectral density of the outputs, $\boldsymbol{S}_{YY} = \{S_{QQ}, S_{\dot{Q}\dot{Q}}\}^T$, is then directly obtained from

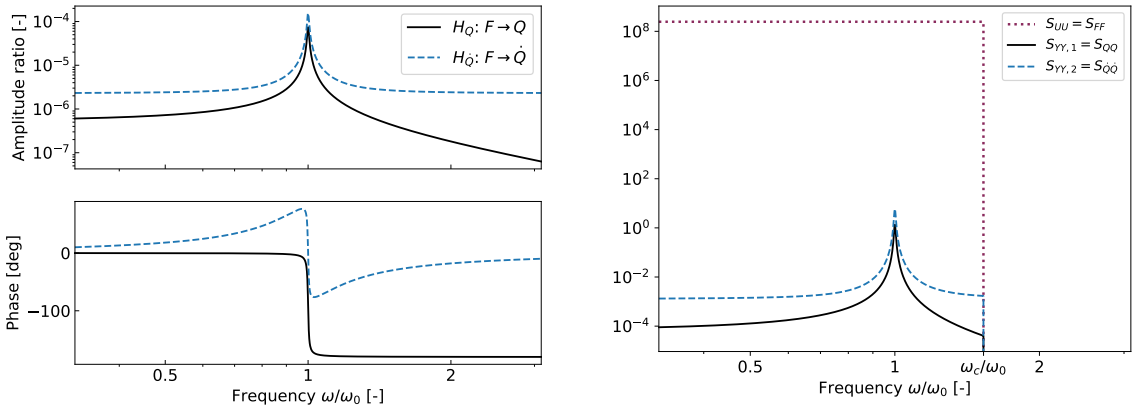

Figure 2. Left: Amplitude and phase (Bode plot) for the components of the transfer function going from the input (force $\boldsymbol{f}$) to the states (position and velocity q and $\dot{q}$). The results are centered around the natural frequency ω_0. Right: Autospectral density of the input and states as obtained using the linear response theory (Equation 8).

the ones of the input by using Equation 8 and Equation 16. The values of $\boldsymbol{S}_{UU}$ and $\boldsymbol{S}_{YY}$ for

this example are illustrated in Figure 2. The standard deviations of the outputs are obtained from Equation 9, giving: $\sigma_Q = 0.033$ m and $\sigma_{\dot{Q}} = 0.146$ m/s. In the next section, it will be shown that in this case, the steady-state PDFs of the states are Gaussian. Therefore, the PDFs can be entirely determined from the mean and standard deviation of the states. The Gaussian distribution obtained from linear theory is plotted in the left of Figure 1 based on the standard deviation mentioned above. Pros and cons of the method are discussed in Section 4.

3.4. FPE

The state-space Itô equation corresponding to Equation 14 with a Gaussian process forcing is obtained from Equation 10 as:

$$\mathrm{d}\boldsymbol{x} = \boldsymbol{f}_\mu(\boldsymbol{x}, \boldsymbol{u})\,\mathrm{d}t + \boldsymbol{\Sigma}\,\mathrm{d}\boldsymbol{W}, \quad \text{with} \quad \boldsymbol{f}_\mu = \begin{bmatrix} \dot{q} \\ -kq/m - c\dot{q}/m + F_0/m \end{bmatrix}, \quad \boldsymbol{\Sigma} = \begin{bmatrix} 0 \\ \sigma_F/m \end{bmatrix} \tag{19}$$

The term $\boldsymbol{f}_\mu$ represents the deterministic part of the equation. In this example, we assume a constant forcing F_0 for this part, whereas the stochastic part of the loading is attributed to $d\boldsymbol{W}$. The associated FPE (Equation 11) is:

$$\frac{\partial p}{\partial t} = -\dot{q}\frac{\partial p}{\partial q} + \frac{\partial}{\partial \dot{q}}\left[\left(\frac{k}{m}q + \frac{c}{m}\dot{q} - \frac{F_0}{m}\right)p\right] + \frac{\sigma_F^2}{2m^2}\frac{\partial^2 p}{\partial \dot{q}^2} \tag{20}$$

where $p(q, \dot{q})$ is the joint probability density of q and $\dot{q}$. From the analysis of the overdamped system (Orstein-Uhlenbeck process), we expect a stationary solution of the form:

$$p(q, \dot{q}) = \frac{1}{\sqrt{2\pi\sigma_Q^2}}\frac{1}{\sqrt{2\pi\sigma_{\dot{Q}}^2}} e^{-\frac{(q-q_0)^2}{2\sigma_Q^2}} e^{-\frac{\dot{q}^2}{2\sigma_{\dot{Q}}^2}} \tag{21}$$

After inserting into Equation 20, and evaluating at $\{q, \dot{q}\} = \{0, 0\}$, and $\{q, \dot{q}\} = \{1, 1\}$, we identify the standard deviation as:

$$\sigma_Q^2 = \frac{\sigma_F^2}{2ck} \tag{22}$$

$$\sigma_{\dot{Q}}^2 = \frac{\sigma_F^2}{2cm} \tag{23}$$

We note that for the stationary solution, there is no correlation between the velocity and position, even if a correlation exists at the initial condition. The PDFs of the individual states are obtained by integration of the joint PDF p in all the other directions but the one of interest, for instance:

$$p_Q(q) = \int_{-\infty}^{\infty} p(q, \dot{q}) d\dot{q} \tag{24}$$

In this simple example, the PDF is a Gaussian and the variables are uncorrelated: $p(q, \dot{q}) = p_Q(q)p_{\dot{Q}}(\dot{q})$. We plot the steady-state solutions of the FPE in Figure 1.

In this work, we implemented a 2D finite-element (FEM) solver to time-integrate the FPE with two state variables, such as Equation 11, but not necessarily linear. In Figure 3, we illustrate how the PDFs of the position and velocity evolve between the initial condition and a time sufficiently large compared to the time scale of the system. As indicated previously, it is seen how the two states become uncorrelated as time evolves. We verified that the steady state solution from our numerical FEM implementation indeed led to the same PDFs and standard deviations as the ones presented in this section.

The results of Section 2.5 can be directly applied to the 2D case presented here. It can be shown that the solution of the Lyapunov equation (Equation 13) is a diagonal matrix, the coefficients of which are given by Equation 22 and Equation 23.

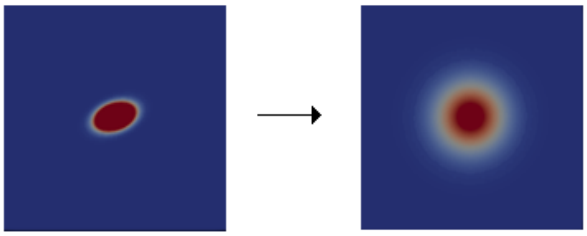

Figure 3. Time evolution of the probability density function of two state variables at the initial time (left) and after the time-integration of the FPE. The states are: position (on the x-axis) and velocity (on the y-axis) of the generalized coordinate for the support-structure bending.

4. Discussions, limitations and path forward

4.1. Advantages and limitations of the stochastic linear theory

The advantage of the stochastic linear theory is in its simplicity, ease of use, computational efficiency, and in the fact that the method can be extended to arbitrary input spectra. Further, the method does not suffer from the "curse of dimensionality" discussed in Section 4.2. In our example, we limited ourselves to a quasi-Gaussian input spectrum, but arbitrary (and more realistic) load spectra can be used.

A downside of the method is that the probability density function is not readily obtainable. The standard deviation can be obtained from the spectrum, but not the higher order moments. If the spectra are assumed to be Gaussian though, the steady-state solution of the FPE that we presented in Section 2.5 can be used to obtain the PDFs of the system states. Therefore, both the probability density function and the spectra of the states can be obtained with linear theory, and the information can be useful to the early design phase of a wind turbine.

Another disadvantage of the method is that nonlinear relationships need to be linearized, which can lead to inaccuracies. For instance, the wind speed is the natural input to the wind turbine system, and it is expected that the loading will have a squared dependency on the wind speed. Such dependency cannot be used explicitly but could be accounted for by introducing additional states that filter the inputs and approximate the nonlinear operation, at the expense of increasing the number of states of the system.

4.1.1. Additional outputs In this work, we have limited our analysis to the determination of the spectrum, statistics, and probability density functions of the system states. In most applications, additional outputs are desired. For instance, the design of wind turbines typically requires the determination of the internal loads of components (e.g., blades or tower). As long as the outputs are functions of the states, accelerations, and inputs of the system (i.e., of the form given in Equation 1), it is possible to include them in the formalism presented in this article. For the linear theory, Equation 8 can be directly used from a linearization of the output equation. For the FPE, the principle consists in augmenting the state vector to include the outputs in it. Formally, we can introduce the augmented state vector $\boldsymbol{x}_{\text{aug}} = \{\boldsymbol{x}, \boldsymbol{u}\}$. The application of the FPE is then identical, replacing $\boldsymbol{x}$ by $\boldsymbol{x}_{\text{aug}}$.

Often, design methodologies rely on time series analyses instead of probabilistic and statistical approaches. For instance, the fatigue of components is estimated by applying the rain-flow counting algorithm on time series of the component stresses [13]. One possible path forward is to generate time series from the knowledge of the autospectral density of the signal and apply the rain-flow counting algorithm on these sampled time series. Linear theory provides such a quantity, but the Fokker-Planck approach only provides the PDF. In any case, applying a sampling method on the outputs, though likely orders of magnitude faster than performing time integrations of the system (due to the leveraging of fast Fourier transform algorithms to

sample from the autospectral density), appears unsatisfactory given our objectives to circumvent sampling. Alternative approaches can consist of modeling the physics of the damage directly into the system using additional states. The downside is that this approach would further increase the number of states of the system, which is undesirable (see Section 4.2). A likely path forward is instead to go away from time-series analyses and rain-flow counting for the estimation of component damage and use a probabilistic and statistical approach. Such an idea can be supported by the fact that the standard deviation is generally accepted to be a good proxy of damage equivalent loads. Further, component failures inherently have a stochastic nature, which often predominates their deterministic counterpart [14]. Last, wind turbine blades tend to fail because of manufacturing defects, which cannot be captured by damage equivalent load. A shift away from time-series damage analysis is therefore encouraged.

4.2. Limitations of the Fokker-Planck approach

In this article, we have shown how the resolution of the FPE can provide the desired probability density functions of the different states of the system for a nonlinear system, such as the ones found in wind energy applications. The stationary solution of the FPE, if existing, is likely to provide the necessary statistics for evaluating the design. It can be obtained with significantly less computational time, as dedicated solvers can be implemented. However, solving the FPE requires a numerical sampling of the state space, and the computational requirement increases with the number of degrees of freedom. Obtaining the tails of the distributions and extreme events requires a wide domain, which further increases the computational requirements. This is referred to as the "curse of dimensionality," that is, the combinatorial growth of variables with the dimension of the problem.

4.3. Potential paths forward

In [15], the authors propose solving the stationary FPE in high-dimensional cases by combining tensor decomposition and Chebyshev spectral differentiation. The tensor decomposition techniques lead to linear growth in the variable numbers with the number of dimensions. The authors demonstrate their approach on several examples, including a nonlinear oscillator with 10 spatial dimensions. The authors of [16] focus on single-dimensional stationary solutions and give a closed-form solution for a generalized FPE. They further give a free-energy-like functional composed of energy and entropic terms and show that the stationary solutions minimize this free-energy functional. Finally, the authors demonstrate that the stationary solution is also the maximizer of a constrained optimization problem where the entropic term is the objective function. While their article is limited to a single spatial dimension, generalizing the entropic terms to multiple dimensions suggests obtaining the stationary solution of the FPE by computing the maximal entropy distribution. Similar methods have proven effective in uncertainty quantification [17] and machine learning [18].

5. Conclusion

Current wind turbine design procedures require multiple time-domain simulations to account for the stochasticity of the environmental conditions. Different random seeds are used to generate time series of turbulent wind and sea states, and these samples are used as input for time-domain simulations. The multiple simulations are used to assess statistical properties, such as the potential damage of individual components or the overall performance of the design. In this work, we investigated ways to avoid the computationally intensive time-domain simulations. We identified two ways to obtain probability density functions (PDFs) and statistical moments of states and outputs without the need for time-domain sampling: stochastic linear theory and the integration of the Fokker-Planck equation (FPE).

Stochastic linear theory provides a means to obtain the spectral density, covariance, and standard deviation of the state and outputs from the spectral density of the inputs. These statistical properties can then be used as proxy to evaluate the fatigue and ultimate loads on the system components. The method can be applied to arbitrary input spectra, but cannot provide the PDFs of the states and outputs. The other limitation resides in the linear assumption, which is only valid close to the operating point of interest.

The integration of the FPE provides the time evolution of the PDFs of the states (and simple outputs). The solution method can be simplified by considering only the steady-state solution of the FPE. The integration of the Fokker-Planck equation still presents some challenges. It requires a form of numerical sampling of the state space, and therefore, the computational requirement increases with the number of degrees of freedom. This is referred to as the "curse of dimensionality." Additionally, the method does not provide the covariance, which could be critical to assess component damage.

In this work, we compared the two approaches with the conventional "brute-force" sampling approach. The proof of concept presented showed promising results and consistency between the two approaches when applied to a linear system. The methods return different quantities of interest; therefore, a combination of the two can be beneficial to estimate component damage and the overall performance of a wind turbine.

Because of the curse of dimensionality, the generalization and implementation of high-fidelity stochastic models of wind turbine design tools would require an involved process. It is nevertheless believed that the methods illustrated here can be applied to canonical systems with few degrees of freedom, to obtain preliminary wind turbine designs during the scoping and bidding phases of a project, where quick evaluations and design turnarounds are required. Future work will focus on presenting more practical applications of the methods to wind turbine designs and study the computational requirements needed as the number of dimensions of the problem increase.

References

[1] International Standard IEC, Workgroup 3, *IEC 61400-3 Wind turbines : Design requirements for offshore wind turbines*. IEC, 2005.
[2] J. Quick, K. Dykes, P. Graf, and F. Zahle, "Optimization under uncertainty of site-specific turbine configurations," *J. of Physics Conference Series*, vol. 753, 2016.
[3] G. Terejanu, P. Singla, T. Singh, and P. D. Scott, "Uncertainty propagation for nonlinear dynamic systems using gaussian mixture models," *J. of Guidance, Control, and Dynamics*, vol. 31, 2008.
[4] O. L. Maitre, O. Knio, H. Najm, and R. Ghanem, "Uncertainty propagation using wiener-haar expansions," *J. of Computational Physics*, vol. 197, 2004.
[5] N. Sahinidis, "Optimization under uncertainty: state-of-the-art and opportunities," *Computers & Chemical Engineering*, vol. 28, 2004.
[6] B. Friedland, *Control System Design: An Introduction to State-Space Methods*. Dover Books on Electrical Engineering, Dover Publications, 2012.
[7] E. Branlard, "Welib, wind energy library, github repository `http://github.com/ebranlard/welib/`, `https://doi.org/10.5281/zenodo.7306075` last accessed november 2022," 2022.
[8] C. Rackauckas and Q. Nie, "DifferentialEquations.jl – A Performant and Feature-Rich Ecosystem for Solving Differential Equations in Julia," *Journal of Open Research Software*, vol. 5, p. 15, May 2017.
[9] E. Vanmarcke, *Random fields: Analysis and synthesis*. The MIT Press, Cambridge, Massachusetts, 1983.
[10] H. Risken and T. Frank, *The Fokker-Planck Equation: Methods of Solution and Applications*. Springer Series in Synergetics, Springer Berlin Heidelberg, 1996.
[11] E. Branlard and J. Geisler, "A symbolic framework for flexible multibody systems applied to horizontal-axis wind turbines," *Wind Energy Science*, vol. 7, no. 6, pp. 2351–2371, 2022.
[12] E. Branlard, "Flexible multibody dynamics using joint coordinates and the Rayleigh-Ritz approximation: The general framework behind and beyond Flex," *Wind Energy*, vol. 22, no. 7, pp. 877–893, 2019.
[13] J. Manwell, E. Branlard, J. McGowan, and B. Ram, *Wind Energy Explained, 3rd edition*. J. Wiley and Sons, LTD, December 2023.

[14] P. S. Veers, "Fatigue crack growth due to random loading," tech. rep., Sandia National Laboratory - Sandia report SAND87 - 2039 - UC 60, 1987.
[15] Y. Sun and M. Kumar, "Numerical solution of high dimensional stationary fokker–planck equations via tensor decomposition and chebyshev spectral differentiation," *Computers & Mathematics with Applications*, vol. 67, no. 10, pp. 1960–1977, 2014.
[16] M. Jauregui, A. L. Lucchi, J. H. Passos, and R. S. Mendes, "Stationary solution and h theorem for a generalized fokker-planck equation," *Physical Review E*, vol. 104, no. 3, p. 034130, 2021.
[17] T. J. Sullivan, *Introduction to uncertainty quantification*, vol. 63. Springer, 2015.
[18] D. M. Blei, A. Kucukelbir, and J. D. McAuliffe, "Variational inference: A review for statisticians," *Journal of the American statistical Association*, vol. 112, no. 518, pp. 859–877, 2017.

Acknowledgements
This work was authored in part by the National Renewable Energy Laboratory, operated by Alliance for Sustainable Energy, LLC, for the U.S. Department of Energy (DOE) under Contract No. DE-AC36-08GO28308. Funding provided by the U.S. Department of Energy Office of Energy Efficiency and Renewable Energy Wind Energy Technologies Office. The views expressed in the article do not necessarily represent the views of the DOE or the U.S. Government. The U.S. Government retains and the publisher, by accepting the article for publication, acknowledges that the U.S. Government retains a nonexclusive, paid-up, irrevocable, worldwide license to publish or reproduce the published form of this work, or allow others to do so, for U.S. Government purposes.